International Journal of Engineering & Technology, 7 (4.14) (2018) 533-537

International Journal of Engineering & Technology

Website: www.sciencepubco.com/index.php/IJET

Research paper

Magnetic Properties of Magnetite Nanoparticles (Fe_3O_4-NPs) Coated with Mesoporous Silica by Surfactant Templated Sol-Gel Method

Nurul Izza Taib[1,2,3]*, Timothy G. St. Pierre[2], Robert C. Woodward[2], Michael J. House[2]

[1]*Faculty of Applied Sciences, Universiti Teknologi MARA, Perak Branch, Tapah Campus, 35400 Tapah Road, Perak, Malaysia*
[2]*School of Physics, The University of Western Australia, Crawley WA 6009, Australia*
[3]*School of Molecular Sciences, The University of Western Australia, Crawley WA 6009, Australia*
**Corresponding author E-mail: izza257@uitm.edu.my*

Abstract

Here, we present the magnetic properties of silica-coated magnetite nanoparticles. We have coated 7 nm of Fe_3O_4 with cetyltrimethylammonium bromide (CTAB) for phase transformation from hydrophobic to hydrophilic. Core-shell structure of silica-coated magnetite nanoparticles have been obtained using surfactant templated sol-gel method. The obtained silica-coated magnetite nanoparticles were characterized by transmission electron microscopy (TEM), fourier transform infrared (FTIR) spectroscopy and superconducting quantum interference device (SQuID). The hysteresis loops of the coated particles were measured using SQuID and the results showed a superparamagnetic behavior at room temperature. The saturation magnetization (M_s) of the coated particles indicate the presence of non-magnetic surface layers resulting from the strong chemical attachment of the silica to the Fe_3O_4's surface, also observed by FTIR spectroscopy.

Keywords: *magnetite, iron oxide nanoparticles, superparamagnetism, silica coating, magnetic properties.*

1. Introduction

Over the past decade, superparamagnetic iron oxide (Fe_3O_4) nanoparticles have drawn significant attention owing to their unique characteristics for various potential biomedical applications [1-3] such as gene [4] and drug delivery, cell labeling and detection [5, 6], magnetically assisted drug delivery [7] and MRI contrast agents [8, 9]. Due to their superparamagnetism, they have played a role as contrast agents in magnetic resonance imaging (MRI) [10]. They offer convenient contrast enhancement in MRI due to their high availability, convenience of the preparation route, biocompatibility and biodegradable nature [1-3].

However, uncoated magnetite nanoparticles are colloidally unstable over long periods due to their tendency to aggregate in order to reduce their free energy. As a result, these aggregation processes significantly decrease their interfacial area, thus resulting in the loss of dispersibility [11]. It is very crucial to chemically stabilize magnetite nanoparticles against degradation during or after the synthetic processes [12].

One of the ways of stabilizing the magnetite nanoparticles is based on a surface functionalization. Silica has been employed for coating oxide nanoparticles as they able form stable, biocompatible shell to help minimise agglomeration [1,3, 13] by screening the magnetic dipolar attraction among the nanoparticles. MCM-41 has been used as a mesoporous structure for the SiO_2 coating, as a result of its regular mesopores, with diameters that can be tailored between 1.5 and 10 nm using different surfactants in the synthesis process. It exhibits a very high surface area, high accessible pore volume, very low toxicity, and good thermal stability [13-15]. The combination of mesoporous silica and iron oxide nanoparticles to prepare magnetic mesoporous silica nanoparticles has been widely exploited due to their potential for simultaneous MRI detection and drug delivery [16-19].

In this work, superparamagnetic iron oxide (Fe_3O_4) nanoparticles were synthesised using the method of Sun et al [20]. The nanoparticles were then used as a core material for the fabrication of mesoporous magnetic nanocomposites. The method involves growing mesoporous silica ($mSiO_2$) directly onto the magnetic nuclei by a surfactant templated sol-gel method.

2. Material and methods

All chemicals were purchased from Sigma-Aldrich unless otherwise stated: benzyl ether (99%), iron (III) acetylacetonate ($Fe(acac)_3$; 97%), oleic acid (BDH, 92%), oleylamine (70%), tetraethyl orthosilicate (TEOS; 98%), hexadecyltrimetyl ammonium bromide (>99%), and ethyl acetate, were used as received.

2.1. Preparation of magnetite (Fe_3O_4) nanoparticles

Magnetite (Fe_3O_4) was synthesized by the organic decomposition of iron(III) acetylacetonate ($Fe(acac)_3$) in benzyl ether at 300 °C, in the presence of oleic acid, oleyl amine, and 1,2-tetradecanediol, as previously described [1]. In brief, $Fe(acac)_3$ (508 mg), 1,2-tetradecandiol (2304 mg), oleic acid (1.69 g) and oleylamine (1.61 g) were added to benzyl ether (10.00 mL). Moisture was removed by heating the solution to 100 ^oC under constant stirring. The mixture was heated to 200 ^oC for 2 hrs and then heated to reflux (~300 ^oC) under an atmosphere of nitrogen for 1 hr. After cooling, the reaction mixture was precipitated in ethanol (40 mL) and centri-

Copyright © 2018 Authors. This is an open access article distributed under the Creative Commons Attribution License, which permits unrestricted use, distribution, and reproduction in any medium, provided the original work is properly cited.

fuged at 3000*g* for 15 minutes to collect a black precipitate. The precipitate was resuspended in hexane (7.50 mL) and centrifuged again under identical conditions. The supernatant containing magnetite nanoparticles was stored under an atmosphere of argon in darkness before further use.

2.2. Preparation of silica-coated magnetite nanoparticles

In a typical procedure, 12.5 mg of iron oxide (Fe_3O_4) were dispersed in 0.50 mL chloroform. The magnetite (0.50 mL) was transferred to 5.00 mL of water by mixing the particles with 100 mg of cetyltrimetyl ammonium bromide (CTAB) solution and the resulting solution was stirred vigorously for 30 minutes. The formation of an oil-in-water microemulsion resulted in a turbid brown solution. Then, the mixture was heated up to 60 ^oC and aged at that temperature for 20 minutes under stirring to evaporate the chloroform, resulting in a transparent black Fe_3O_4-CTAB solution. In order to create a $mSiO_2$ coating layer around the Fe_3O_4-CTAB, the resulting solution was added to a mixture of 43 mL of water and 350 µL of 2.00 M NaOH solution and the mixture was further heated up to 70 ^oC under stirring. Then, 500 µL of tetraethylorthosilicate (TEOS), and 3.00 mL of ethylacetate was added to the reaction solution in sequence under rapid stirring. The solution was further heated for 2 hrs to give rise to a light brown precipitate. After cooling, a light brown solid product was isolated by centrifugation and washed three (3) times with ethanol to remove the unreacted species and dried in air. The surfactant template (CTAB) was removed from the mesopore channels by refluxing the as-synthesized materials in alcoholic solutions of ammonium nitrate (20 mg/mL) at 60 ^oC for 30 minutes. The obtained light brown solid was allowed to cool down, centrifuged, and washed three times (3) with ethanol and finally dried in air. The above treatment was performed a total of three (3) times before further application.

2.3. Characterization methods

Transmission electron microscopy was performed on samples using the JEOL 2100 electron microscope operated at 120 kV. Fe_3O_4, Fe_3O_4-CTAB, and silica-coated magnetite nanoparticles suspensions were pipetted onto continuous 200-mesh carbon-coated copper grids and left to dry in air for a few hours before commencing the measurements. The prepared nanoparticles were further characterized with ATR-FTIR (Perkin Elmer Spectrum One FT-IR spectrometer).

The magnetic measurements used throughout this work were performed on a Quantum Design MPMS SQuID VSM. Samples were prepared by compressing 10 mg of nanoparticles into gel capsules. Samples were mounted within a brass holder and connected to one end of a sample rod that is inserted into the dewar. The other end is attached to a stepper motor that is used to position the sample within the center of the SQUID pickup coils.

This experiment involves measuring the magnetization, *M*, of the sample as a function of the applied magnetic field, *H*. It is often referred to as the *M-H* loop. The samples were cooled from room temperature to 5 K in zero-field. Hysteresis loops were subsequently measured at 5 K by sweeping the field up to +70 kOe, then to -70 kOe and finally back to +70 kOe. The field spacing was 1 kOe on these sweeps. Hysteresis loops were measured at higher temperatures by warming at the completion of the lower temperature loop.

3. Results and discussions

3.1. Transmission electron microscopy (TEM)

For all core-shell structures investigated here, Fe_3O_4-NPs from the same batch have been used as the magnetic core. The surface morphology and silica shell thickness of silica-coated magnetite nanoparticles were analyzed with TEM. Fig. 1 (a) and (b) show typical TEM images from representative Fe_3O_4-NPs in hexane, and Fe_3O_4-CTAB in water. TEM analysis shows that the Fe_3O_4-NPs and Fe_3O_4-CTAB prepared are monodisperse, spheroidal in shape with a mean particle size of 7 nm with a standard deviation of 0.7 nm.

Subsequently, the Fe_3O_4-NPs were coated with mesoporous silica ($mSiO_2$) by hydrolysis of TEOS with the sol-gel method under basic conditions. The hydrophobic Fe_3O_4-NPs dispersed in chloroform were transferred to an aqueous phase by using cetyltrimethylammonium bromide (CTAB) as stabilizing agents and porous structure-directing agent to yield Fe_3O_4–CTAB. In this process, the solution became black when iron oxide particles were mixed with CTAB, showing the successful production of water-dispersable Fe_3O_4–CTAB. TEM images in Fig. 1 (b) show that the size of particles remains unchanged even after coating with CTAB.

Fig. 2 represent silica coated magnetite nanoparticles with 45 nm silica shell thickness. The thickness value was measured from the edge of dark core to the edge of surface of silica.

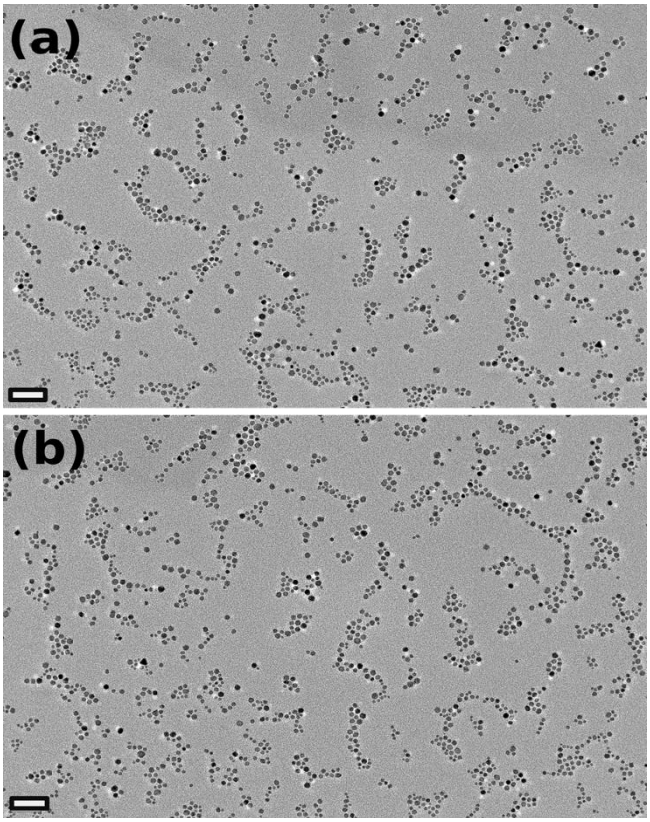

Fig. 1: TEM micrograph of the nanoparticles: (a) Fe_3O_4-NPs and (b) Fe_3O_4-CTAB. Scale bars: (a) and (b) 50 nm

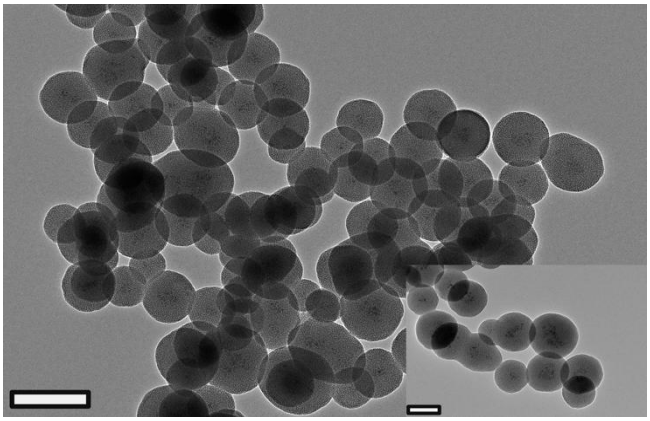

Fig. 2: TEM micrograph of silica-coated magnetite nanoparticles: Scale bars: 200 nm (insets: 100 nm).

A minimum 55 particles of each samples were measured and the data reported as the average of thickness. The TEM images showed that the coated nanoparticles were spherical in shape with an average diameter of 136 nm. It shows the distribution of iron oxide nanoparticles (multiple darker spots) within the silica matrix (grey area). The diameter value was measured from edge to edge of surface of silica. A minimum 55 particles of each samples were measured and the data reported as the average of diameter.

3.2. Fourier transform infrared (FTIR) spectroscopy

The obtained silica-coated magnetite nanoparticles were refluxed in an ethanol solution of NH_4NO_3 in order to remove the CTAB template. Fig. 3 (a) depicts FTIR spectra of template free of silica coated magnetite nanoparticles. The absence of -CH_2- stretching bands at 2975 cm^{-1} and 2926 cm^{-1} and -CH_2- bending at 1456 cm^{-1}, Fig. 3 (b), in the samples suggests successful CTAB removal via solvent extraction [21].

The appearance of absorption bands at 1090 and 800 cm^{-1} are attributed to the presence of asymmetric and symmetric stretching bands of -Si-O-Si-. The peaks at 960 and 1635 cm^{-1} are associated with the Si-O-Si stretching vibration of surface Si-OH groups and physisorbed water, respectively [21, 22]. In addition, the IR peak at 570 cm^{-1} and 375 cm^{-1} corresponding to the stretching vibration of Fe-O bond [23] contributes to the weak band in the all samples, indicating the presence of iron oxide.

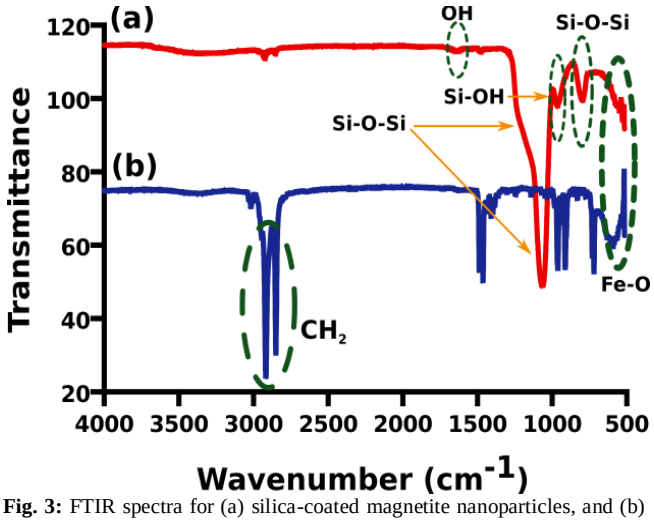

Fig. 3: FTIR spectra for (a) silica-coated magnetite nanoparticles, and (b) Fe_3O_4-CTAB nanoparticles.

3.3. Magnetic properties

Fig. 4 (a) shows the magnetization curve of Fe_3O_4-NPs, showing superparamagnetic behaviour at room temperature and hysteretic behaviour at 5K. The saturation magnetization for the Fe_3O_4-NPs was relatively high (103.4 emu/g of Fe_3O_4 at 5K). This was reduced to 89.4 emu/g of Fe_3O_4 at 300K. The coercivity at 5K was ≈ 0.15 kOe with no measureable coercivity at 300K.

As could be seen from Fig. 6, Fe_3O_4-CTAB, and silica-coated magnetite nanoparticles show superparamagnetic behaviour at room temperature with no hysteresis. The Fe_3O_4-CTAB and silica-coated magnetite nanoparticles had saturation magnetization at 5K of 96.7 and 52.1 emu/g of Fe_3O_4, respectively. This was reduced to 82.4 and 43.4 emu/g of Fe_3O_4 at 300K. The coercivity of Fe_3O_4-CTAB at 5K was ≈ 0.26 and absent at 300K. Meanwhile, the coercivity was reduced to ≈ 0.15 kOe for silica coated magnetite nanoparticles, and was again absent at 300K.

Meanwhile, ZFC/FC curves reveal that the T_B for Fe_3O_4-NPs (Fig. 4 (b)) and Fe_3O_4-CTAB (Fig. 7 (a)), are approximately at 60 K for both. This was reduced to 46 K for silica-coated magnetite nanoparticles (Fig. 7 (b)).

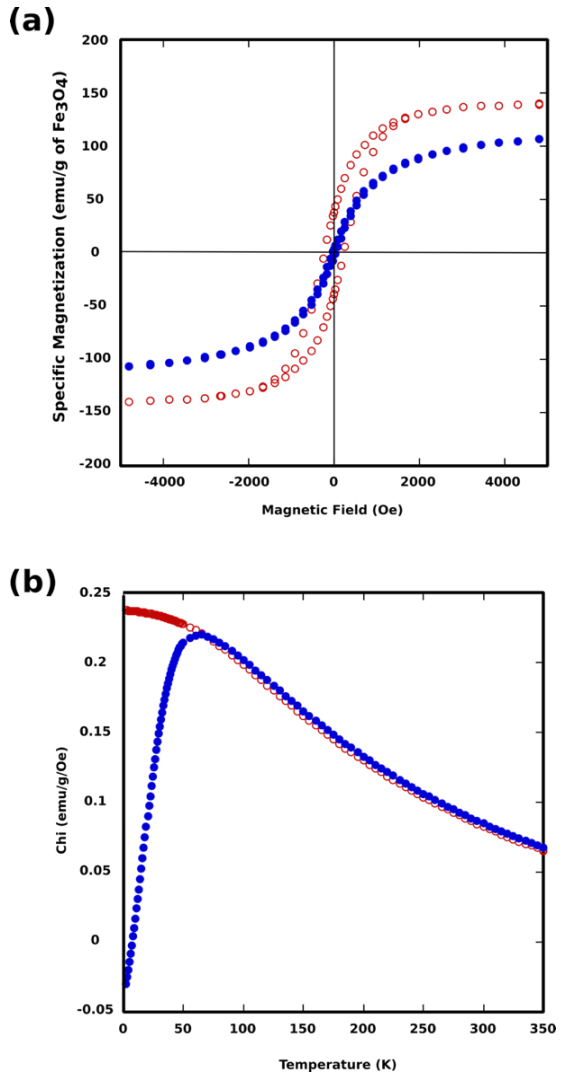

Fig. 4: (a) The magnetization curves for Fe_3O_4-NPs shows at 5K (red circles) and 300K (blue dots) and (b) Zero-field cooled (blue dots)-field cooled (red circles) curves are coincident above ca. 60K for Fe_3O_4-NPs.

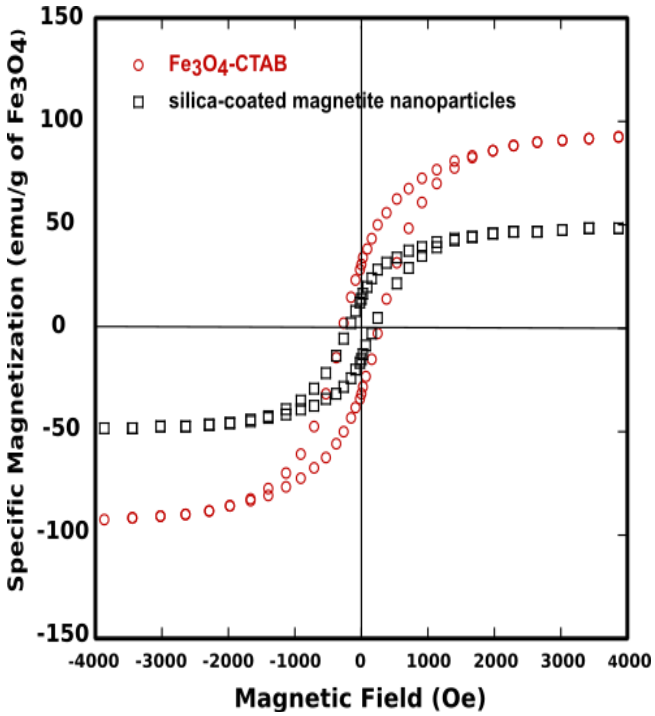

Fig. 5: The magnetization curves at 5K for Fe_3O_4-CTAB and silica-coated magnetite nanoparticles.

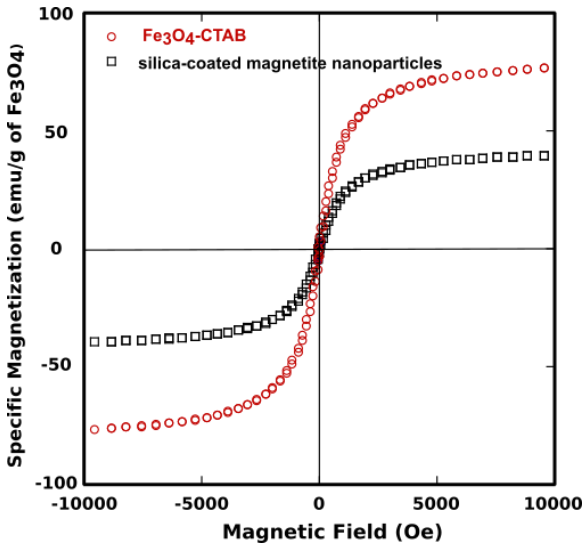

Fig. 6: The magnetization curves at 300K for Fe_3O_4-CTAB and silica-coated magnetite nanoparticles.

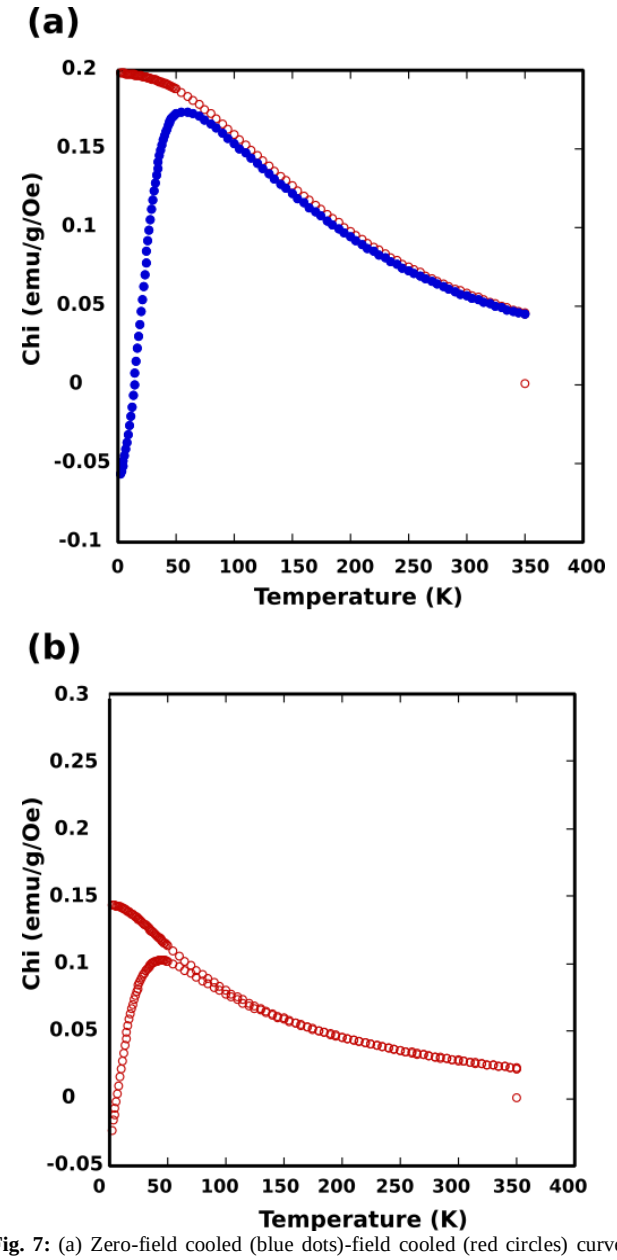

Fig. 7: (a) Zero-field cooled (blue dots)-field cooled (red circles) curves are coincident above ca. 60K for Fe_3O_4-CTAB. (b) Zero-field cooled field cooled curves for silica-coted magnetite nanoparticles

The reduced saturation magnetization of Fe_3O_4-NPs compared with bulk magnetite (92 emu/g of of Fe_3O_4) [24, 25] is most likely due to the increase in surface area/volume ratio and therefore spin canting effects at the surface [26]. Thermal fluctuations will significantly reduce the total magnetic moments at a given field when the energy of a magnetic particle becomes comparable to the thermal energy [27]. The presence of silica coating results in a lower saturation magnetization (M_s) of silica-coated magnetite nanoparticles than that of the Fe_3O_4-NPs. This might result from the coating of silica on the core surface, which might quench the magnetic moment [25, 28].

4. Conclusion

In this work, we successfully synthesized Fe_3O_4-NPs by thermal decomposition method, and coated them with mesoporous silica. The coated nanoparticles were found to be spherical in TEM images with a core shell structure with an average diameter of 136 nm with silica shell thickness of 45 nm. A decrease in M_s and in T_B value was found indicating the presence of silica coating on the surface of Fe_3O_4-NPs. The silica-coated magnetite nanoparticles exhibit superparamagnetic behaviour at room temperature with a saturation magnetization, M_s of 89.4 emu/g of Fe_3O_4. We expect that the superparamagnetism properties of coated nanoparticles will make it a good candidate for magnetic targeting drug delivery and as contrast agent for Magnetic Resonance Imaging (MRI).

Acknowledgement

The authors acknowledge Universiti Teknologi MARA (UiTM), Malaysia and Ministry of Higher Education, Malaysia (600-IRMI/MyRA5/3/LESTARI (048/2017), Australian Research Council and The University of Western Australia in providing the fund. The microscopy analysis was carried out using facilities at the Centre for Microscopy, Characterisation and Analysis, The University of Western Australia, which are supported by University, State and Federal Government funding.

References

[1] Mahmoudi M, Sant S, Wang B, Laurent S & Sen T (2011), Superparamagnetic iron oxide nanoparticles (SPIONs): development, surface modification and applications in chemotherapy. *Advanced Drug Delivery Review* 63, (1-2), 24-46.

[2] Qiao R, Yang C & Gao M (2009), Superparamagnetic iron oxide nanoparticles: from preparations to in vivo MRI applications. *Journal of Materials Chemistry* 19, 6274-6293.

[3] Pankhurst QA, Connolly J, Jones SK & Dobson J (2003), Applications of magnetic nanoparticles in biomedicine. *Journal of Physics D: Applied Physics* 36, R167-R181.

[4] Scherer F, Anton M, Schillinger U, Henke J, Bergemann C, Kruger A, Gansbacher B & Plank C (2002), Magnetofection: enhancing and targeting gene delivery by magnetic force in vitro and in vivo. *Gene Therapy* 9, 102-109.

[5] Chou LY, Ming K & Chan WC (2011), Strategies for the intracellular delivery of nanoparticles. *Chemical Society Reviews* 40(1), 233-245.

[6] Lee ESM, Shuter B, Chan J, Chong MSK, Ding J, Teoh SH, Beuf O, Briguet A, Tam KC, Choolani M & Wang SC (2010), The use of microgel iron oxide nanoparticles in studies of magnetic resonance relaxation and endothelial progenitor cell labelling. *Biomaterials* 31(12), 3296-3306.

[7] Rejinold NS, Thomas RG, Muthiah M, Lee HJ, Jeong YY, Park I-K & Jayakumar R (2016), Breast Tumor Targetable Fe_3O_4 Embedded Thermo-Responsive Nanoparticles for Radiofrequency Assisted Drug Delivery. *Journal of Biomedical Nanotechnology* 12(1), 43-55.

[8] Chouly C, Pouliquen D, Lucet I, Jeune JJ & Jallet P (1996), Development of superparamagnetic nanoparticles for MRI: effect of particle size, charge and surface nature on biodistribution. *Journal of Microencapsulation* 13(3), 245-255.

[9] Carroll MR, Woodward RC, House MJ, Teoh WY, Amal R, Hanley TL & Pierre TS (2010), Experimental validation of proton transverse relaxivity models for superparamagnetic nanoparticle MRI contrast agents. *Nanotechnology* 21(3), 035103.
[10] Chen D-X, Sun N, Huang Z-J, Cheng C-M, Xu H & Gu H-C (2010), Experimental study on T_2 relaxation time of protons in water suspensions of iron-oxide nanoparticles: Effects of polymer coating thickness and over-low $1/T_2$. *Journal of Magnetism and Magnetic Materials* 322(5), 548-556.
[11] Liu J, Qiao SZ, Hu QH & Lu GQ (2011), Magnetic nanocomposites with mesoporous structures: synthesis and applications. *Small* 7(4), 425-443.
[12] Corma A (1997), From Microporous to Mesoporous Molecular Sieve Materials and Their Use in Catalysis. *Chemical Reviews* 97, 2373-2419.
[13] Vogt C, Toprak MS, Muhammed M, Laurent S, Bridot J-L & Muller RN (2010), High quality and tuneable silica shell-magnetic core nanoparticles. *Journal of Nanoparticle Research* 12, 1137-1147.
[14] Taylor KML, Kim JS, Rieter WJ, An H, Lin W & Lin W (2008), Mesoporous Silica Nanospheres as Highly Efficient MRI Contrast Agents. *Journal of American Chemical Society* 130(7), 2154-2155.
[15] Yi DK, Selvan ST, Lee SS, Papaefthymiou GC, Kundaliya D & Ying JY (2005), Silica-Coated Nanocomposites of Magnetic Nanoparticles and Quantum Dots. *Journal of American Chemical Society* 127(14), 4990-4991.
[16] Lee JE, Lee N, Kim H, Kim J, Choi SH, Kim JH, Kim T, Song IC, Park SP, Moon WK & Hyeon T (2010), Uniform mesoporous dye-doped silica nanoparticles decorated with multiple magnetite nanocrystals for simultaneous enhanced magnetic resonance imaging, fluorescence imaging, and drug delivery. *Journal of American Chemical Society* 132(2), 552-557.
[17] Ye F, Laurent S, Fornara A, Astolfi L, Qin J, Roch A, Martini A, Toprak MS, Muller RN & Muhammed M (2012), Uniform mesoporous silica coated iron oxide nanoparticles as a highly efficient, nontoxic MRI T_2 contrast agent with tunable proton relaxivities. *Contrast Media & Molecular Imaging* 7, 460-468.
[18] Zhang C, Wangler B, Morgenstern B, Zentgraf H, Eisenhut M, Untenecker H, Kruger R, Huss R, Seliger C, Semmier W & Kiessling F (2007), Silica-and alkoxysilane-coated ultrasmall superparamagnetic iron oxide particles: a promising tool to label cells for magnetic resonance imaging. *Langmuir* 23, 1427-1434.
[19] Liong M, Lu J, Kovochich M, Xia T, Ruehm SG, Nel AE, Tamanoi F & Zink JI (2008), Multifunctional inorganic nanoparticles for imaging, targeting, and drug delivery. *ACS Nano* 2(5), 889-896.
[20] Sun S, Zeng H, Robinson DB, Raoux S, Rice PM, Wang SX & Li G (2004), Monodisperse MFe_2O_4 (M = Fe, Co, Mn) Nanoparticles. *Journal of American Chemical Society* 126(1), 273-279.
[21] Taib NI, Endud S & Katun MN (2012), XRD, FTIR and ^{13}C CP/MAS NMR Studies of Composite comprising Poly(vinyl acetate)-silylated Si-MCM-41. *Advanced Materials Research* 364, 159-163.
[22] Sangok FE, Yahaya SM, Taib NI, Sa'ad SZ & Rasaruddin NF (2012), Comparison Study of Amino-Functionalized and Mercaptopropyl-Functionalized Mesoporous Silica MCM-41. *Advanced Materials Research* 550-553, 1603-1606.
[23] Nasrazadani S & Raman A (1993), The application of infrared spectroscopy to the study of rust systems—II. Study of cation deficiency in magnetite (Fe_3O_4) produced during its transformation to maghemite (γ- Fe_2O_3) and hematite (α-Fe_2O_3). *Corrosion Science* 34(8), 1355-65.
[24] Y, Lee J, Bae CJ, Park J-G, Noh H-J, Park J-H & Hyeon T (2005), Large-Scale Synthesis of Uniform and Crystalline Magnetite Nanoparticles Using Reverse Micelles as Nanoreactors under Reflux Conditions. *Advanced Functional Materials* 15(3), 503-509.
[25] Zaitsev VS, Filimonov DS, Presnyakov IA, Gambino RJ & Chu B (1999), Physical and Chemical Properties of Magnetite and Magnetite-Polymer Nanoparticles and Their Colloidal Dispersions. *Journal of Colloid and Interface Science* 212, 49-57.
[26] Linderoth S, Hendriksen PV, Bodker F, Wells S, Davies K, Charles SW & Morup S (1994), On spin-canting in maghemite particles. *Journal of Applied Physics* 75, 6583-6585.
[27] Shafi KVPM & Gedanken A (1998), Sonochemical Preparation and Size-Dependent Properties of Nanostructured $CoFe_2O_4$ Particles. *Chemistry of Materials* 10(11), 3445-3450.
[28] van Leeuwen DA, van Ruitenbeek JM, de Jongh LJ, Ceriotti A, Pacchioni G, Haberlen OD & Rosch N (1994), Quenching of magnetic moments by ligand-metal interactions in nanosized magnetic metal clusters. *Physical Review Letters* 73(10), 1432-1435.